



Ni/nano-TiO₂ composite electrodeposits: Textural and structural modifications

S. Spanou, E.A. Pavlatou*, N. Spyrellis¹

Laboratory of General Chemistry, School of Chemical Engineering, National Technical University of Athens, 9 Heron Polytechniou Str., Zografos Campus, Athens GR-15780, Greece

ARTICLE INFO

Article history:

Received 31 December 2007

Received in revised form 26 June 2008

Accepted 28 June 2008

Available online 6 July 2008

Keywords:

Nickel electrodeposition

Composite coating

Titania

Preferred orientation

Nano-particles

ABSTRACT

Nanocomposite coatings were obtained by electrochemical codeposition of TiO₂ nano-particles (mean diameter 21 nm) with nickel, from an additive-free Watts type bath. The electrodeposition of Ni-TiO₂ composites was carried out on a rotating disk electrode (RDE), by applying direct current. Pure Ni deposits were also produced under the same experimental conditions for comparison. The surface morphology, the crystallographic orientation of nickel matrix and the grain size of the deposits were investigated, along with the distribution and the percentage, of the embedded nano-particles in nickel matrix, as a function of pH, current density and concentration of TiO₂ nano-particles in the bath. The observed textural modifications of composite coatings are associated with specific structural modifications of Ni crystallites provoked by the adsorption-desorption phenomena occurring on the metal surface, induced by the presence of TiO₂ nano-particles. It has been observed that the presence of TiO₂ nano-particles favours the [100] texture of nickel matrix. Moreover, the codeposition of titania nano-particles with nickel was found to be favoured at low pH and low applied current values. As the titania incorporation percentage is increased, a considerable grain refinement in the nanometer region was revealed followed by an improvement of the quality of the nickel preferred orientation.

© 2008 Elsevier Ltd. All rights reserved.

1. Introduction

Metal matrix composite coatings containing TiO₂ particles exhibit interesting photoelectrochemical and photocatalytical behaviour [1–3] accompanied by improved mechanical properties [4–8]. Especially, Ni matrix composites reinforced by TiO₂ micro- [7,9–10], submicron- [10,11] and nano-particles [1,4–6,10,12–14] can be successfully synthesized by electrodeposition utilizing either sulfamate or Watts plating baths.

The codeposition of nanoscaled particles within an electroplating process is an attractive procedure to produce improved materials for microtechnological applications [4]. The principal parameters acting on the composite electrodeposition process are the compositions of the electrolytic bath [15], the presence of additives [15–17], the pH value [15,18], the temperature [15], the induced hydrodynamic conditions, the imposed current conditions [8] and of course the characteristics of the reinforcing particles (size [10], conductivity [19], hydrophilicity/hydrophobicity [20] and surface charge [15,21]). It is important to adjust the plating variables in order to control the properties of the produced composite coatings that depend on the amount of incorporated particles and their

distribution in the metal matrix, as well as, on the microstructural characteristics of the metal matrix.

Research related to Ni-TiO₂ composite coatings has demonstrated that the codeposition percentage of nano-titania particles is difficult to be controlled quantitatively, because the particles are frequently agglomerated in the metal matrix, as well as in the electrolyte [10,13] due to their significant high surface energy. Given that TiO₂ particles seems to incorporate in a limited extend compare to other ceramic particles, like SiC particles in example [9], the major challenges are the enhancement of particles incorporation accompanied by their uniform distribution in the deposit. It should be mentioned that the highest amount of nano-titania embedded particles does not exceed ~3.5 vol.% [13] in the presence of organic additives by using Watts type bath. In addition, the major published reports realised the production of Ni-nano-TiO₂ composite coatings by using additives and only few have addressed the synthesis from an additive-free Watts bath [1,4]. It is noticeable that the presence of organic additives in the bath introduces new parameters that influence the codeposition process and consequently increases the complexity of the electrochemical phenomena.

Taking into consideration all the above mentioned data, we have conducted a comprehensive study in an extended area, regarding the influence of the electrolytic parameters on the codeposition process. Specifically, we investigated the effect of TiO₂ loadings in bath, applied current density and pH value, on the surface mor-

* Corresponding author. Tel.: +30 210 7723110, 7723130; fax: +30 210 7723088.

E-mail address: pavlatou@chemeng.ntua.gr (E.A. Pavlatou).

¹ ISE member.

phology, crystal size and the preferred orientation of the deposits in correlation with the quantity of embedded nano-TiO₂ particles.

2. Experimental

Pure Ni and composite Ni–TiO₂ coatings were electrolytically deposited from an additive-free nickel Watts solution under conditions described in Table 1. The electrodeposition experiments were performed on rotating disk electrode (RDE) with a constant rotation velocity of 600 rpm under direct current conditions. The solution temperature was maintained by water circulation at a thermostated temperature of 50 ± 1 °C. Nickel plate of 99.9% purity, positioned on the side of the electrolytic cell, was used as a soluble anode and a standard calomel electrode served as a reference electrode. The initial pH of the bath was adjusted to constant values in the range of 1–4.5. The TiO₂ powder (Degussa P25) with a mean diameter of 21 nm was used as received without any pre-treatment. This commercial powder was prepared by the aerosil process, and is frequently used in photocatalytic studies and consists by a mixture of the crystalline phases of anatase and rutile. TiO₂ particles were maintained in an electrolytic bath in suspension by continuous magnetic stirring of 320 rpm for at least 24 h before deposition as well as, during electrolysis. The load of particles in the electrolyte was set at 20, 50 and 100 g/L and the applied current density varied from 0.5 to 40 A/dm². All the experiments were conducted by using a Wenking PGS 95 Potentio–Galvanoscan. The substrates were brass discs with a total surface area of 0.05 dm² that were mechanically polished in order to eliminate the epitaxial influence on the structure of deposits and chemically cleaned in an ultrasonic agitated bath before deposition. After electrolysis, the deposits were ultrasonically cleaned in distilled water for 10 min in order to remove any loosely adsorbed TiO₂ particles from the surface. The thickness of the produced coatings was at least 40 μm in order to obtain preferred orientations fully developed and therefore permit their determination in such a way to attain results comparable and reliable.

X-ray diffraction analysis was carried out using a Siemens D-5000 diffractometer, with a Cu Kα radiation. Diffractograms were recorded with a step size of 0.02° for 2θ ranging from 20 to 160° and measuring time 1 s per step. In order to describe the structure and estimate quantitatively the preferred orientation of the nickel deposits, the relative texture coefficient (RTC_(hkl)) was calculated, which is defined as:

$$RTC_{(hkl)} = \frac{I_{hkl}/I_{hkl}^0}{\sum_1^6 I_{hkl}/I_{hkl}^0} \times 100\%$$

where I_{hkl} are the diffraction intensities of the (hkl) lines measured in the diffractogram of the deposit and I_{hkl}^0 are the corresponding

intensities of a standard Ni powder sample randomly oriented. The summation in the denominator is taken for the six “basic” lines visible in the diffraction pattern, i.e., (100), (200), (220), (311), (331) and (420). A preferred orientation through an axis [hkl] is indicated by values of $RTC \geq 16.67\%$ and the strength of the preferred orientation is maximum when RTC approaches the value of 100% [22].

Grain size of the crystallites was determined by using the (200) and (220) X-ray diffraction peak broadening according to the Scherrer equation. The full-width-half-maxima (FWHM) of the peaks were estimated after background correction and subtracting the instrumental line broadening, which was calculated using a standard Ni random oriented powder according to the Warren equation;

$$B^2 = B_M^2 - B_S^2$$

where B_M is the measured diffraction FWHM peak and B_S is the broadening of Ni standard powder sample [22]. The standard Ni powder was randomly oriented with a mean grain size of 0.5 μm.

Scanning electron microscopy (SEM) and high-resolution field emission SEM (HRFE-SEM) was applied in order to study the structure, morphology and composition of the surface and the cross-sectional profile of the Ni–TiO₂ coatings. Depth profiles of the composites were obtained by using glow discharge optical spectroscopy (GDOS) in order to extract information about the distribution of the components versus the coating thickness. The concentration of TiO₂ particles on the surface was evaluated by using fluorescence X-ray spectroscopy (XRF). These values were verified also by energy dispersive X-ray spectroscopy (EDS) measurements.

Experiments were carried out to determine the pH variation of the bath at various initial pH values in the presence of two different loads of titania in order to investigate the adsorption–desorption phenomena of H⁺ taking place on the surface of titania particles. The batches of oxide were added and kept in suspension by magnetic stirring at a concentration of 20 and 100 g/L in a 200-cm³ cell containing 100 cm³ of the used Watts type solution. The initial pH of the solution was adjusted to the required value using NH₃ or HNO₃ solution. The pH was modified after titania addition, and reached a steady-state value after 2 h mixing [23] that was recorded.

3. Results and discussion

3.1. Influence of nano-TiO₂ particles on nickel electrocrystallization

3.1.1. Pure Ni deposits

The electrocrystallization of Ni is known to be a highly inhibited process as a consequence of hydrogen codeposition. Depending on plating conditions, mainly pH value of the bath and current density, Amblard et al. observed a predominance of a definite inhibitor, which selectively promotes one mode of growth and leads to a deposit exhibiting specific structural characteristics. It has been established that nickel deposits from an additive-free Watts type bath under direct current conditions exhibit three inhibited textures [1 1 0], [2 1 0] and [2 1 1] attributed to the presence of atomic, molecular forms of adsorbed hydrogen and colloidal Ni(OH)₂ in the catholyte interface, respectively. Moreover, the observed [1 0 0] mode of growth is considered to be the most “free” from inhibiting chemical species [24–27].

The estimation of the preferred crystal orientation based on the X-ray diffraction diagrams of pure nickel deposits from an additive-free Watts bath resulted to the stability diagram (Fig. 1a) of textures as a function of pH and current density. The obtained results are in

Table 1

Overview of the electrodeposition parameters for preparation of pure Ni and composite Ni–TiO₂ coatings

Electrolyte composition	
NiSO ₄ ·6H ₂ O	330 g/L
NiCl ₂ ·6H ₂ O	35 g/L
H ₃ BO ₃	40 g/L
TiO ₂ powder Degussa P25 ($d_m = 21$ nm)	20, 50 and 100 g/L
Electrodeposition conditions	
pH	1, 2, 3, 3.5, 4 and 4.4
Temperature (°C)	50
Substrate	Brass disc (diameter 25 mm)
Cathode rotation rate (ω)	600 rpm
Anode	Ni foil
Current density (A/dm ²)	0.5, 1, 2, 5, 10, 20 and 40
Type of current	Direct (DC)
Magnetic stirring (rpm)	320

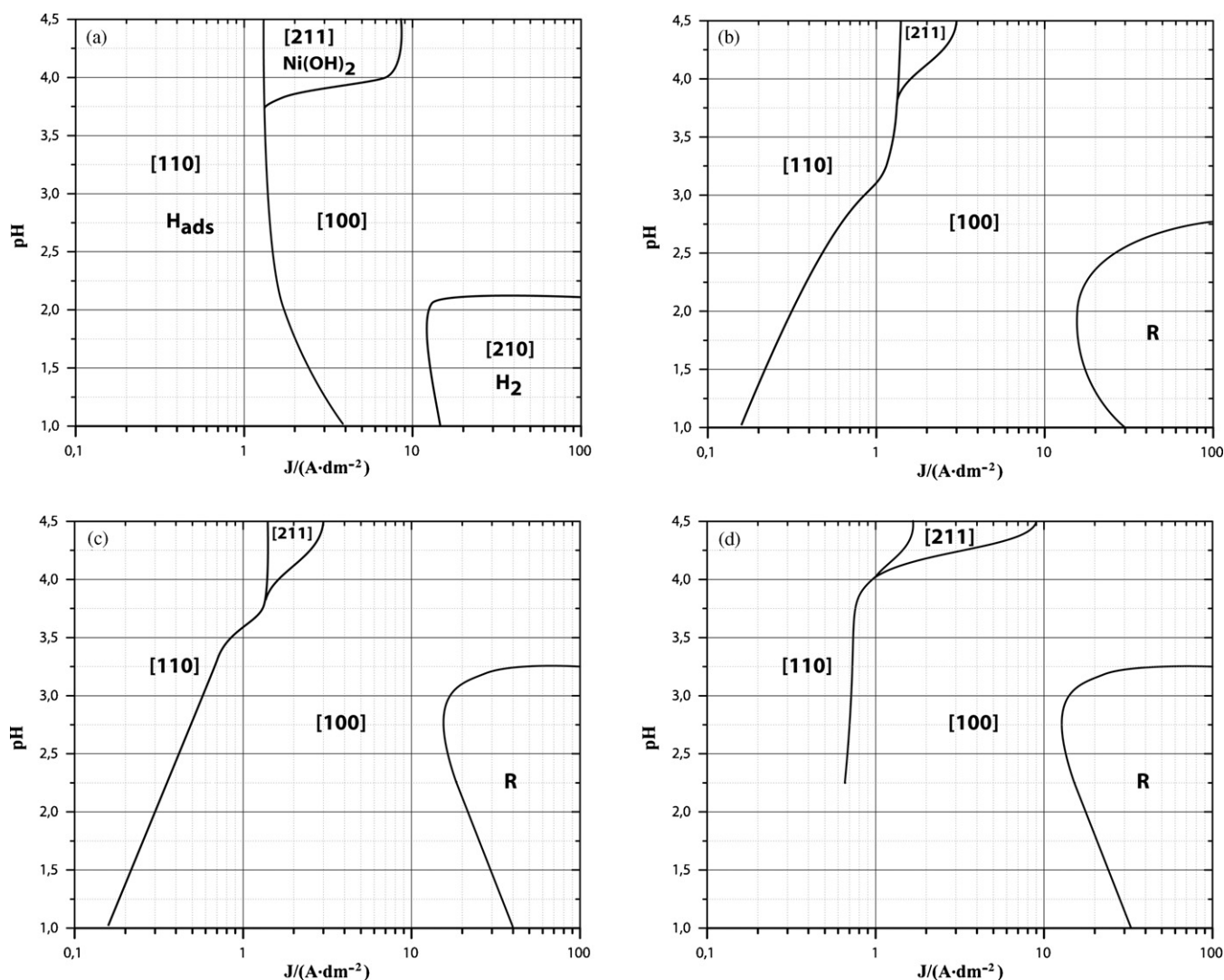


Fig. 1. Stability diagrams of crystal preferred orientations as a function of pH and applied current density of (a) pure Ni and Ni-TiO₂ composites at (b) 20 g/L, (c) 50 g/L and (d) 100 g/L TiO₂ loads in the bath.

accordance with textural modifications reported in literature given that the cathode rotation speed is different. This diagram consists of four domains: (a) at low current densities and an extended region of pH values the [110] preferred orientation of Ni crystallites is favoured, (b) at medium current densities and a broaden region of pH values a [100] texture is observed, (c) at medium current densities and less acidic baths a [211] texture is stabilised and (d) at high current densities and strong acid media a [210] texture is favoured. It should be noticed that the usage of other baths such as chloride, sulfamate, etc. leads to completely different crystal structures under fixed electrodeposition conditions (temperature, current density, pH, etc.) [28].

The structural and morphological characteristics of pure nickel deposits that exhibit the four discrete crystal preferred orientations according to the plating conditions described in Fig. 1a are demonstrated in Fig. 2. In detail, Fig. 2a shows the pseudo-pentagonal crystal symmetry typical for a nickel deposit oriented through the [110] axis; Fig. 2b illustrates the characteristic binary symmetry of [211] oriented crystals; Fig. 2c presents nickel crystals oriented through [100] axis composing long fibres with twins that end up to the shape of tetragonal pyramids and Fig. 2d exhibits the peculiar structure of [210] oriented nickel crystallites [27]. Moreover, the

comparison of SEM images (Fig. 2) indicates that the mean grain size of the four modes of crystal growth varies. As can be observed deposits presenting a [100] texture exhibit the highest mean grain size.

3.1.2. Composite Ni/TiO₂ deposits

Embedding of TiO₂ particles in the nickel matrix provokes changes in the structure of pure nickel coatings with increasing concentration of TiO₂ nano-particles in the electrolyte (Fig. 1b–d). In detail, the region of [100] oriented deposits is expanded with increasing amounts of titania in the bath, accompanied by a confinement of the [211] and [110] domains. Additionally, a transformation of [210] preferred orientation – stable at high current densities and low pH conditions for pure Ni deposits – to randomly oriented crystallites is observed in the presence of TiO₂ nano-particles.

According to literature data the codeposition of oxides with nickel results to textural modifications compare to those observed for pure nickel deposits and seems to be correlated to the loading of the particles in the bath [29,30], the size [10] and surface properties of the dispersoids [18,23]. Thus, it can be concluded that the adsorption–desorption phenomena taking place in the region of the

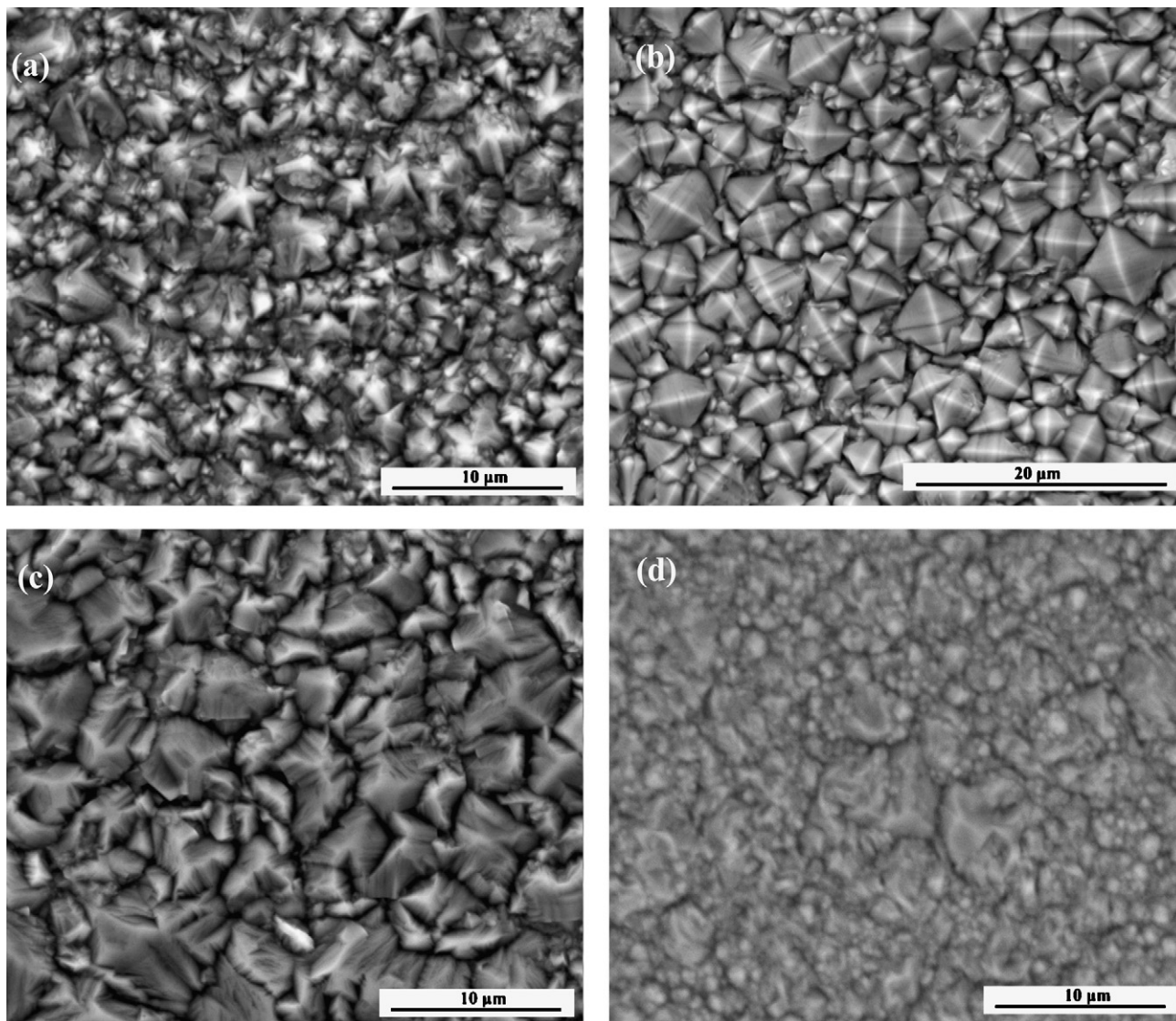


Fig. 2. SEM surface micrographs presenting the typical morphology of pure Ni crystallites oriented through (a) [1 1 0], (b) [2 1 1], (c) [1 0 0] and (d) [2 1 0] axis. The regions of operation conditions under which these typical modes of growth are prepared are shown in Fig. 1a.

catholyte area seem to be changed when surface charged oxides arrive at the cathode and are loosely adsorbed or even partially submerged onto the growing nickel grains.

In this context, addition of titania nano-particles in the bath followed by low current densities and pH values leads to the replacement of [1 1 0] preferred orientation to [1 0 0] texture (Fig. 1). This alteration implies a less intense inhibition of the Ni crystal growth process, as the free mode growth [1 0 0] is favoured. Moreover, the domain of [1 1 0] texture is further confined at medium pH values and low current densities with increasing concentration of the nano-particles in the bath. The observed textural modification could be correlated to the reduced concentration of H_{ads} inhibitors in the catholyte area under the specific electrodeposition conditions induced by the presence of charged TiO_2 nano-particles in catholyte area.

At high pH values and low to medium current densities the region of deposits oriented through [2 1 1] axis is reduced and replaced by composites exhibiting [1 0 0] texture as titania loading in the bath is increased (Fig. 1). This observation indicates that the formation of $Ni(OH)_2$ on the cathode surface is reduced due to the presence of TiO_2 particles in the nickel/catholyte interface.

In contrast, the high incorporation of titania in the metallic matrix at high current densities and low pH values exerts a much more intense inhibition to the Ni crystal growth compared to pure nickel deposits oriented through [2 1 0] axis, leading to the formation of random oriented deposits (Fig. 1). It should be mentioned that the [2 1 0] preferred orientation exhibits a “helical” peculiar structure consisting of a compact connection by edges of tetrahedra with conservation of a common crystallographic direction type [2 1 0] [31]. This texture could be considered as very sensitive to its development and therefore could be also destroyed by the presence of titania nano-particles. Additionally, the region of random oriented deposits expands with increasing content of nano-particles in the electrolyte. Overall, all the textural modifications could be attributed to the adsorption of inhibiting species on the surface of TiO_2 nano-particles. These specific adsorption phenomena could result in a diminution of the activity of the inhibitors affecting the nickel grains growth and thus imposing the free [1 0 0] texture.

Representative XRD patterns of nickel coatings produced at different TiO_2 loadings in the electrolyte are presented in Fig. 3. The diffractograms are characterised by mainly two diffraction peaks (2 2 0) and (2 0 0), which correspond to [1 1 0] and [1 0 0] preferred

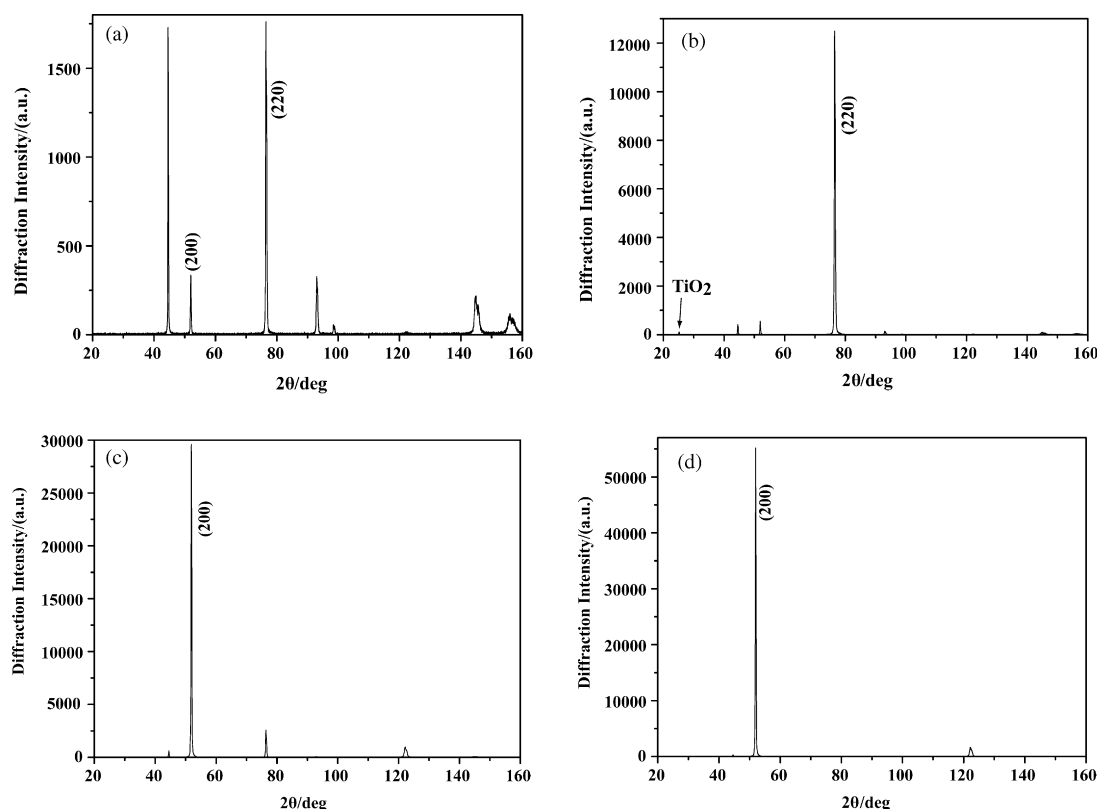


Fig. 3. X-ray diffraction patterns of Ni coatings with various TiO_2 concentrations in the electrolyte prepared under pH 3.5 and $J = 1 \text{ A/dm}^2$: (a) pure Ni deposit and Ni- TiO_2 composite coatings from bath containing (b) 20 g/L, (c) 50 g/L and (d) 100 g/L TiO_2 .

orientation. It should be noticed that the reflection at $2\theta = 25.3^\circ$ could be assigned to the (1 0 0) plane of anatase and cannot be clearly observed due to the relatively high intensity of nickel diffraction peaks (Fig. 3b). A change in relative intensity of the nickel diffraction peaks occurred with increasing amounts of titania in the electrolyte, which could be expressed through the value of the relative texture coefficient of each crystalline orientation. In detail, in the case of pure Ni deposits the XRD diagram is characterised by a strong (2 2 0) diffraction line, together with a weak (2 0 0) line (Fig. 3a), which switches to an intense (2 2 0) line for 20 g/L TiO_2 in the electrolyte (Fig. 3b). Further addition of titania in the bath leads to an exceptional (2 0 0) diffraction line (Fig. 3c and d). The $\text{RTC}_{(hkl)}$ of each (hkl) diffraction line of these deposits is presented in Fig. 4. There is a significant improvement of the quality of the preferred

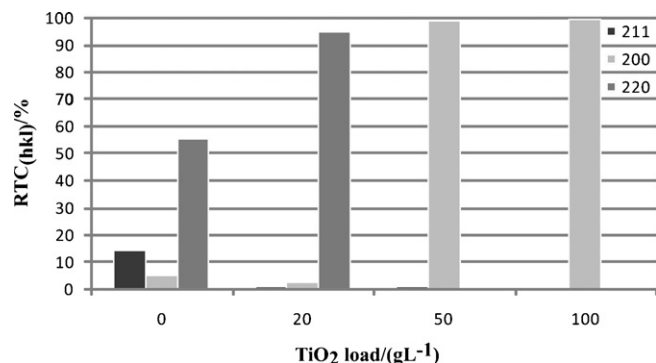


Fig. 4. Relative texture coefficient values of (2 1 1), (2 0 0) and (2 2 0) diffraction lines of Ni coatings with various TiO_2 concentrations in the electrolyte prepared under pH 3.5 and $J = 1 \text{ A/dm}^2$.

orientation by increasing the content of TiO_2 nano-particles in the electrolyte, for example in the case of (2 2 0) lines and the corresponding [1 1 0] texture, the RTC is increased from 55.3% to 94.4% by just adding 20 g/L TiO_2 in the bath (Fig. 4).

Fig. 5 demonstrates the surface morphology of the four deposits described in the X-ray diffraction data of Figs. 3 and 4. Under these plating conditions a pure Ni polycrystalline deposit is produced oriented through [1 1 0] axis with clear borders of the grains (Fig. 5a). With the first addition of TiO_2 nano-particles in the electrolytic bath, the borders of the grains become fuzzy and the mean grain size is reduced compared to pure Ni (Fig. 5b). As mentioned above, the preferred orientation of this composite deposit is preserved and its quality is improved significantly (Fig. 4). By further addition of nano-particles in the bath, the texture of the deposit is switched from [1 1 0] to [1 0 0] and a typical cauliflower surface morphology is observed (Fig. 5c and d). The strength of this preferred orientation is further enhanced at the highest titania loading in the bath (Fig. 4). It is noteworthy that EDS measurements on the surface of these three composites disclosed an increase of the codeposition percentage of the nano-particles in the deposit by increasing the loading in the electrolyte (i.e., 3.75 vol.% for 20 g/L to 7.3 vol.% for 100 g/L).

3.2. Quantitative analysis of the amount of TiO_2 in the composite coatings

From the evaluation of the XRF results it was found that as the concentration of TiO_2 nano-particles in the electrolyte increases, the percentage of TiO_2 nano-particles occluded in the electrodeposit (Fig. 6) is also increased independently from the pH and applied current value. This result is in good correlation with reports

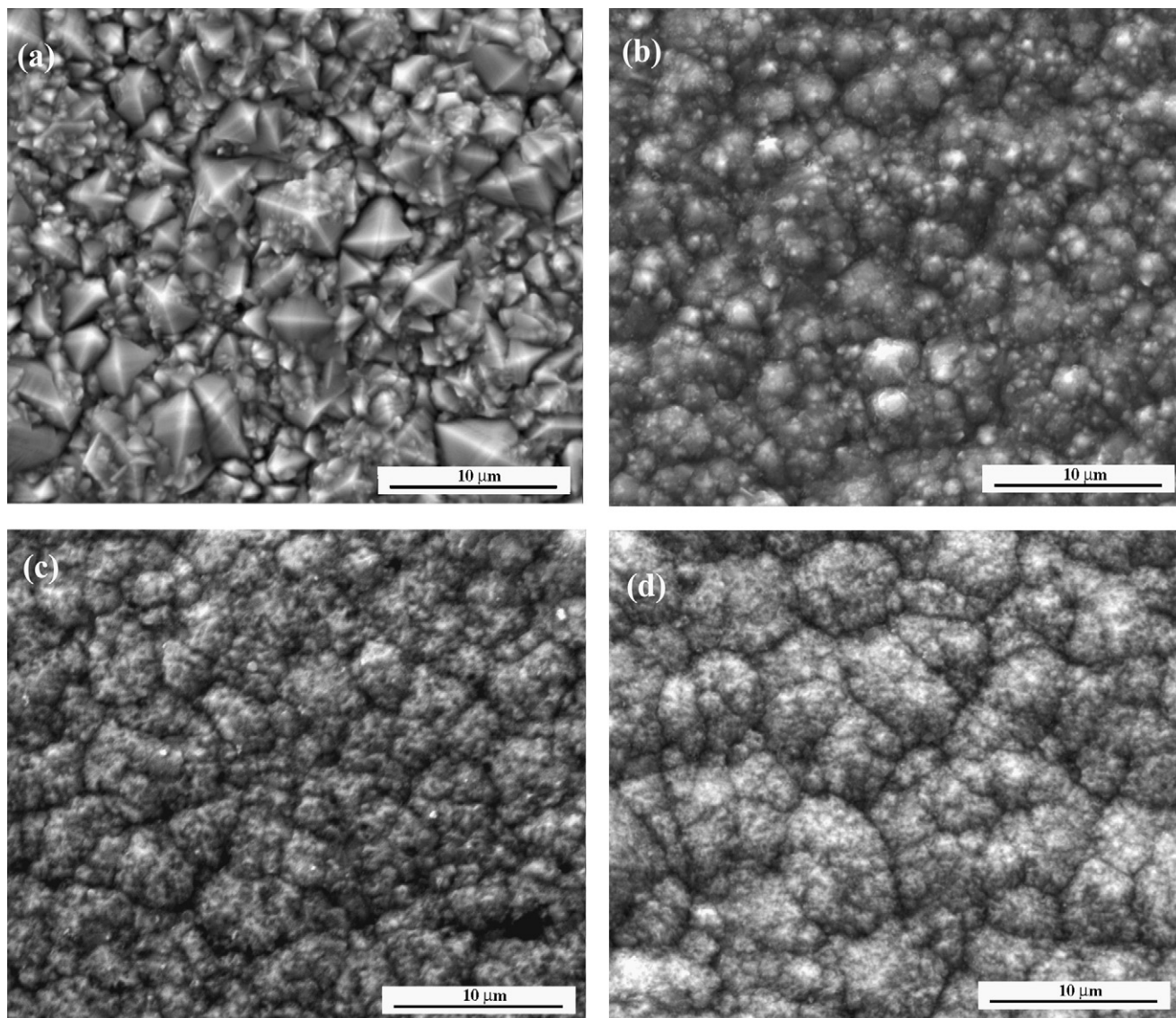


Fig. 5. SEM surface micrographs of (a) pure Ni deposit with a [1 1 0] preferred orientation and Ni-TiO₂ composite coatings with (b) [1 1 0], (c) [1 0 0], and (d) [1 0 0] preferred orientation from bath containing 20 g/L, 50 g/L and 100 g/L TiO₂, respectively. All the coatings were prepared under pH 3.5 and $J = 1 \text{ A/dm}^2$.

related to the study of the TiO₂ nano-particles incorporation in Ni matrix electrodeposits under different values of applied current density [5,13].

However, the codeposition percentage of TiO₂ nano-particles decreases by increasing the pH value at a constant value of current density (Fig. 6a). It seems that codeposition is favoured at low pH values implying that TiO₂ nano-particles are more positively surface charged [15] compare to high bath pH values. On the other hand, at a constant value of pH, the incorporation percentage increases by decreasing current density value (Fig. 6b). According to Fransaer et al., a particle “group” will be engulfed by the growing metal when brought in contact with an electrode with enough foothold to remain on the electrode. A situation that could give this opportunity to the particles to be efficiently embedded in the matrix could be achieved at low current densities [32]. Moreover, Banovic et al. [30], as well as Chen et al. [33] proposed that increasing the number of effective collisions between the oxide particles and the cathode surface per unit volume of deposited matrix will increase the amount incorporated into the coating. According to them, this can be accomplished by using a slower plating rate,

i.e., lower current density, or increasing the number of particles suspended in the electrolyte.

Additionally, the experimental data of this work have revealed that there is a correlation between the concentration of the codeposited nano-particles and the grain size of nickel matrix (Fig. 7). In particular, as the TiO₂ loading in the electrolyte increases under constant values of pH and current density, the TiO₂ vol.% in electrodeposit is also increased (see also Fig. 6), while the mean grain size of the crystallites decreases (Fig. 7a). It should be noticed that this observation stands as long as there is no modification in the texture of the deposits due to an increase of embedded nano-particles into the Ni matrix. While, when the pH and the TiO₂ loading in the bath are constant, the concentration of TiO₂ in deposit decreases and the mean grain size increases by increasing the current density (Fig. 7b). A similar behaviour was reported by studies related to the electro-codeposition of alumina in nickel matrix [30]. It is noteworthy to mention that the maximum incorporation percentage of the nano-particles in the Ni matrix (9 vol.%) has been achieved at low current densities and low pH values (Fig. 7b). The highest amount of nano-titania embedded particles reported

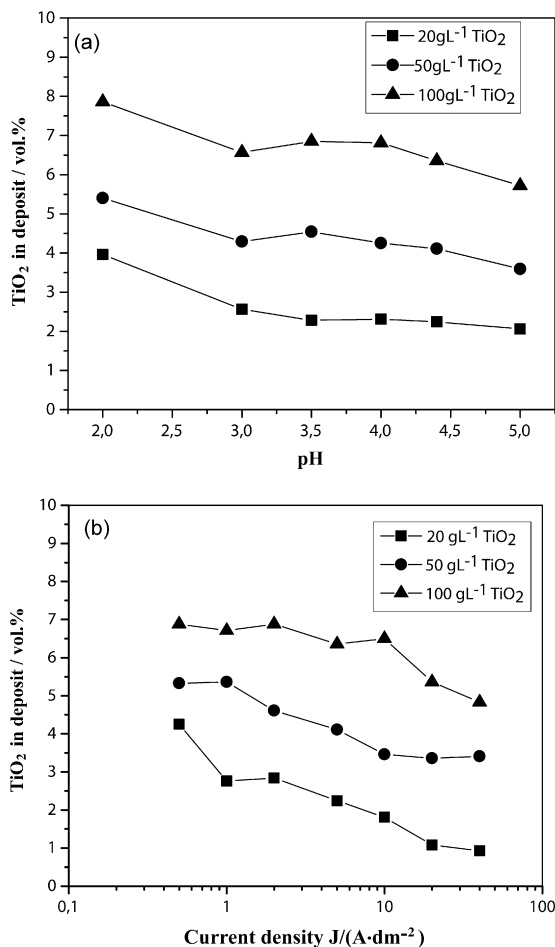


Fig. 6. Volume percentage of nanosized TiO₂ particles in the composite coating at different TiO₂ loadings as a function of (a) pH and constant value of current density $J = 5 \text{ A/dm}^2$ and (b) current density and at constant pH value of 4.4.

in literature does not exceed the $\sim 3.5 \text{ vol.}\%$ by using Watts type bath, though in presence of organic additives [10]. Moreover, at the conditions under which the highest incorporation of titania nano-particles is achieved the mean grain size of composite coatings crystallites is approximately 20 nm. Pure nickel deposits exhibit for the same [100] preferred orientation with the composite a minimum grain size of $\sim 45 \text{ nm}$. Therefore, the embedding of titania nano-particles yields to a considerable nickel grain refinement in the nanoscale region under specific electrolytic conditions (titania loading, pH and current density) compared to pure nickel deposits. This grain downsize of electrodeposited composites is defined by the competition between nucleation and crystal growth [34]. However, the ascription of the observed grain refinement is not yet well defined. Studies concerning the incorporation of TiO₂ nano-particles in nickel have shown that the dispersed nano-particles either increase the nucleation [5] or restrain the crystal size rather by inhibiting crystal growth than by providing new nucleation surfaces [10].

The experimental findings by applying SEM and HRFE-SEM techniques have demonstrated that the distribution of the TiO₂ nano-particles on the surface is uniform without serious problems of agglomeration (Fig. 8a). It seems that the incorporation of the titania nano-particles takes place between the grains as denoted in Fig. 8b. Finally, Fig. 9 presents the cross-sectional SEM micrograph of Ni–TiO₂ revealing a compact composite with a good adhesion with the substrate, while a representative GDOS profile discloses

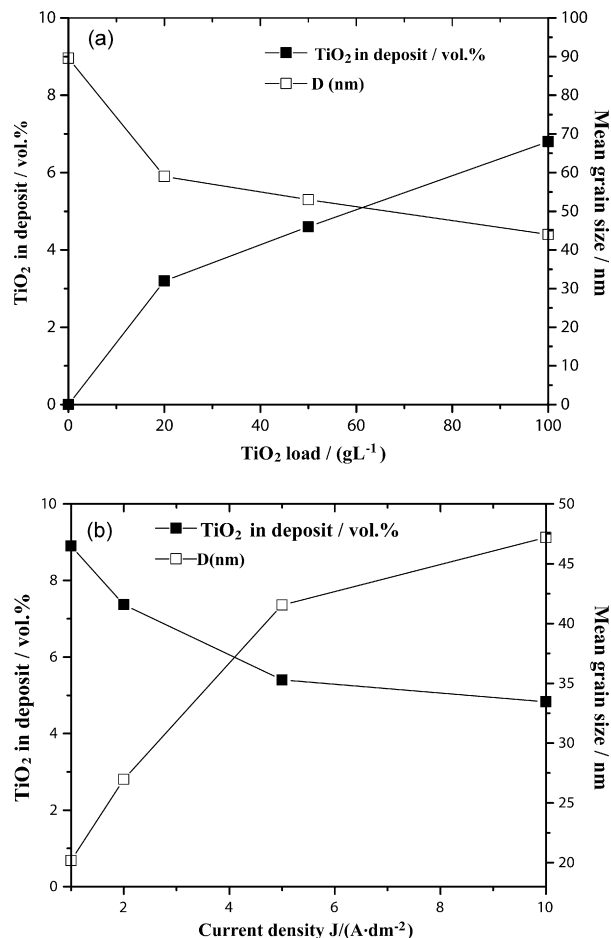


Fig. 7. Variation of vol.% TiO₂ content in the composite coatings Ni crystallites mean grain size as a function of (a) concentration of the titania particles dispersed in the electrolyte at pH 3.5 and $J = 2 \text{ A/dm}^2$ and (b) applied current density versus at pH 2 and 50 g/L TiO₂ in the bath.

the uniform distribution of titania nano-particles in the depth of the deposit (Fig. 10).

3.3. Particle reactivity with H⁺

In order to interpret the observed textural modifications of Ni matrix induced by the presence of TiO₂ particles in the deposits, the nano-particles reactivity with charged ions in the electrolytic bath and especially with H⁺ has been examined. It is known that in electroplating metal-oxide composite coatings, it is necessary to investigate the effects of adding the metal oxide to the electrolyte on resulting electrolyte pH [29]. It has been shown [23,35] that the pH change which occurs, in aqueous solution, after oxide particle addition, depends on the acid–base properties of the powders and indicates the magnitude of the H⁺ exchange on their surface. Fig. 11 shows the change in pH (noted ΔpH) caused by TiO₂ addition into nickel Watts type baths at different pH values and various titania loadings in the bath. After introducing the oxide powders an increase in the bath pH occurred (zone I), and at specific pH value no change is observed after powder addition ($\Delta \text{pH}_{3.5} \cong 0$). This pH is dependent on the load of the powder in the solution and is characteristic for each oxide usually called as point of zero charge (PZC). At pH values larger than the PZC point, a negative change in pH occurred (zones II and III). According to literature data [23,36], a positive change in pH can be interpreted as an adsorption of protons on the powder surface which becomes partially hydroxylated

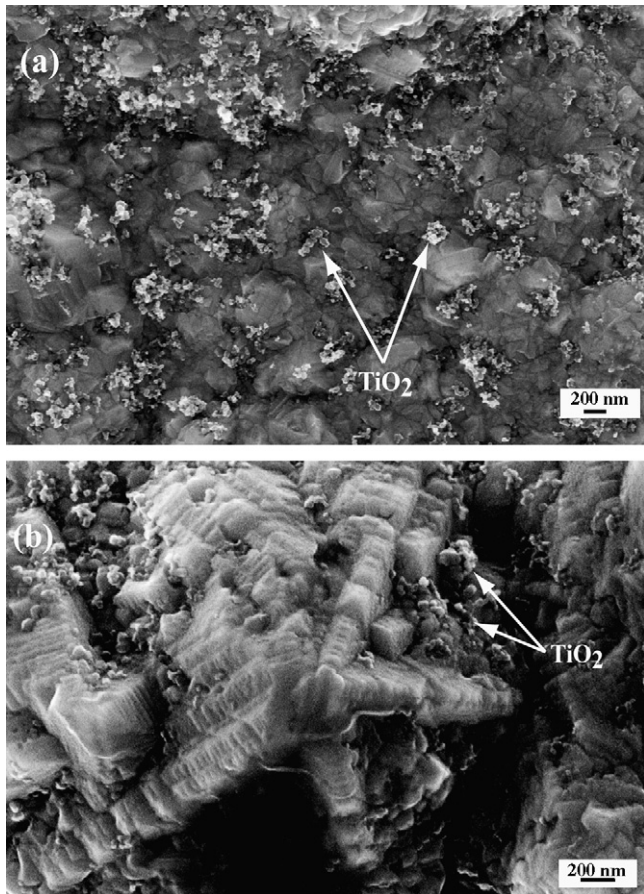


Fig. 8. HRFE-SEM surface micrographs of Ni-TiO₂ composite coatings: (a) a composite coating produced at pH 4.0, $J = 10 \text{ A/dm}^2$ and 100 g/L TiO₂ loading indicating a good distribution of the nano-particles with Ni crystal oriented through [1 0 0] axis and (b) characteristic shape of Ni crystals oriented through [1 1 0] axis produced at pH 3.5, $J = 0.5 \text{ A/dm}^2$ and 100 g/L TiO₂ loading in the bath.

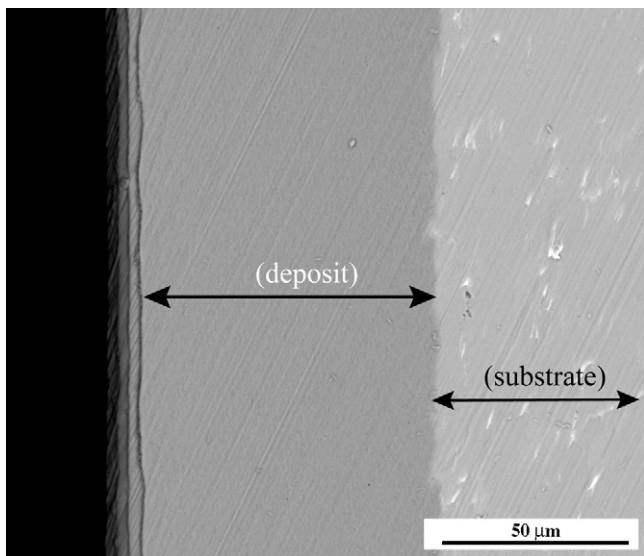


Fig. 9. SEM micrograph of Ni-TiO₂ coating in cross-section. The deposit was produced at pH 3.5, $J = 1 \text{ A/dm}^2$ and 50 g/L TiO₂ in the bath. The codeposition percentage of titania reaches the value of 5.5 vol.%.

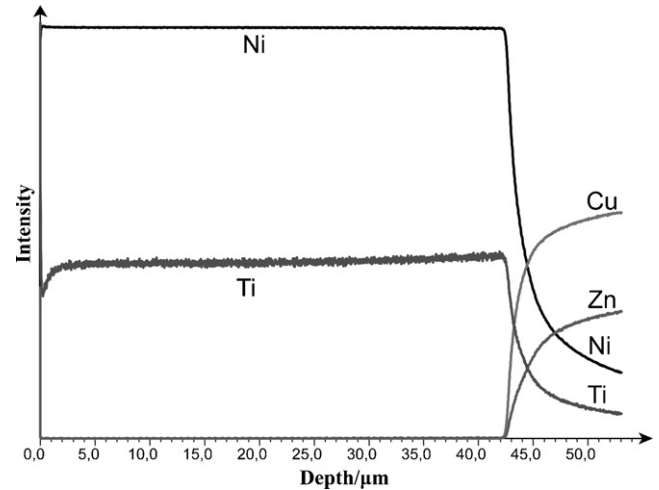
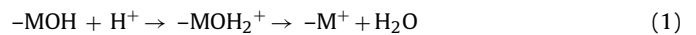


Fig. 10. GDOS depth profile for a Ni-TiO₂ composite prepared on brass discs under pH 3.5, $J = 0.5 \text{ A/dm}^2$ and 100 g/L TiO₂ in the bath. The codeposition percentage of titania remains almost constant across the depth of the deposit at the value of 7.7 vol.%.

according to the following reaction:



In contrast, a decrease in bath pH occurs when particles tend to release protons into the solution, owing to the following reaction:



In the present case, the results obtained show the relationship between the degree of acceptance or release of a proton by the oxide group and the load of the powder in the solution. Specifically, higher concentration of TiO₂ in the electrolyte leads to a higher H⁺ exchange with the solution.

Our experimental data revealed a replacement of [1 1 0] preferred orientation to [1 0 0] under low current densities and low to medium pH values in presence of titania nano-particles in the composites. This textural modification is provoked by the proton adsorption on the titania particle surfaces according to Eq. (1), which inhibits the formation of H_{ads} at the cathode/catholyte interface that impose the [1 1 0] mode of nickel growth. It should be noticed that this inhibition takes place to such an extent that the metallic surface is less hindered by any adsorbed chemical species related to hydrogen codeposition and thus, a [1 0 0] free mode of growth is favoured. Additionally, in the case of very acidic baths and high current densities, the adsorption of H⁺ on the titania particles provokes a local alkalization of the cathode/electrolyte interface

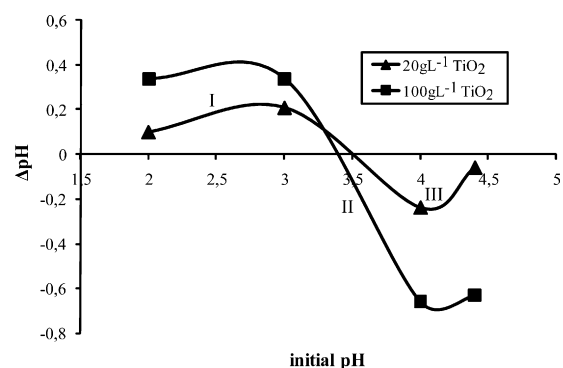


Fig. 11. Variation of initial pH value for an additive-free Watts type bath as a function of concentration of TiO₂ nano-particles in the bath.

produced by the partially hydroxylated layer around the particles as denoted in Eq. (1). Such situation indicates that hydrogen evolution is restrained to some extent and consequently the [2 1 0] preferred crystalline orientation is diminished. In addition, the sensibility of [2 1 0] texture should be taken into account, where the presence of titania nano-particles on the {1 1 1} twins could lead to the destruction of [2 1 0] structure [31].

On the other hand, when the pH is higher than the PZC, titania particles tend to release protons in the bath (Eq. (2)) resulting to a local decrease of pH in the catholyte area, which in turns frustrates the formation/precipitation of Ni(OH)₂ that inhibits every mode of growth except [2 1 1]. Therefore, the region of deposits oriented through [2 1 1] axis, obtained at high pH values and low to medium current densities, is reduced and replaced by composites exhibiting [1 0 0] texture during progressive addition of TiO₂ nano-particles in the bath. Overall, the experimental data revealed that codeposition of TiO₂ nano-particles is favoured at low pH values and current densities, implying that there is a plentiful adsorption of H⁺ on the titania surface and as the particle surfaces become positively charged they will be strongly adsorbed on the cathode leading to an enhanced electrolytic codeposition. Similar results were reported also for the case of Ni/yttria [29] and Zn/titania modified silica [18] composite coatings.

4. Conclusions

The objective of this study was to investigate the effect of TiO₂ nano-particles on the structure of the nickel matrix, putting emphasis on the correlation between inhibition and its effect on morphological features of electrodeposits under an extended region of electrodeposition conditions such as pH of the bath, current density and TiO₂ loading.

With increasing amounts of TiO₂ nano-particles in the bath, the incorporation of TiO₂ nano-particles into nickel matrix was found to modify significantly the texture of the deposits compared to pure Ni coatings under the same pH and applied current density values. Specifically, a confinement of the [2 1 1] and [1 1 0] preferred orientation domains was observed followed by the predominance of [1 0 0] texture over an extended region of electrodeposition conditions. Additionally, a transformation of [2 1 0] preferred orientation to random oriented crystallites is observed in the presence of TiO₂ nano-particles. Based on the observed textural modifications and the pH changes of the bath in the presence of the dispersed powder, it was concluded that H⁺ adsorption–desorption phenomena on the titania surface take place depending on the pH of the electrolyte that finally lead to the inhibition of the reactivity of specific chemical species, which impose specific modes of nickel crystal growth.

As the particle concentration increases from 0 to 100 g/L, the content of the TiO₂ particles in the nano-composite coatings is increased reaching the maximum incorporation percentage of 9 vol.% achieved at low current densities and low pH values. The concentration of the codeposited particles affects the grain size of metal crystallites and the quality of the preferred crystal ori-

entation. In detail, as the TiO₂ nano-particles vol.% in the deposit increases the mean grain size of the nickel matrix decreases and the relative texture coefficient of each texture is improved, resulting in the production of a nanostructured nickel matrix in the range of ~20 nm. TiO₂ nano-particles in the composite coatings are dispersed uniformly in the nickel matrix on the surface as well as, through the cross-section of the deposits and the incorporation of the nano-particles take place between the grains. Concluding, the experimental data proved that is possible to enhance the incorporation of titania nano-particles in a nanostructured nickel matrix by applying low pH and current density values.

Acknowledgement

The authors would like to acknowledge greatly Dr. Manfred Baumgärtner for providing us the HRFE-SEM and GDOS measurements.

References

- [1] N.R. de Tacconi, C.A. Boyles, K. Rajeshwar, *Langmuir* 16 (2000) 5665.
- [2] K. Uii, T. Fujita, N. Koura, F. Yamaguchi, *J. Electrochem. Soc.* 153 (2006) C449.
- [3] T. Deguchi, K. Imai, H. Matsui, M. Iwasaki, H. Tada, S. Ito, *J. Mater. Sci.* 36 (2001) 4723.
- [4] C. Jakob, F. Erler, R. Nutsch, S. Steinhauser, B. Wielage, A. Zschunke, *Proc. 15th Interfinish World Congr and Exhibition, Garmisch-Partenkirchen, 13–15 Sept., 2000.*
- [5] J. Li, Y. Sun, X. Sun, J. Qiao, *Surf. Coat. Technol.* 192 (2005) 331.
- [6] T. Lampke, A. Leopold, D. Dietrich, G. Alisch, B. Wielage, *Surf. Coat. Technol.* 201 (2006) 3510.
- [7] C.S. Lin, C.Y. Lee, C.F. Chang, C.H. Chang, *Surf. Coat. Technol.* 200 (2006) 3690.
- [8] C.T.J. Low, R.G.A. Wills, F.C. Walsh, *Surf. Coat. Technol.* 201 (2006) 371.
- [9] N. Guglielmi, *J. Electrochem. Soc.* 119–8 (1972) 1009.
- [10] T. Lampke, B. Wielage, D. Dietrich, A. Leopold, *Appl. Surf. Sci.* 253 (2006) 2399.
- [11] V.O. Nwoko, L.L. Shreir, *J. Appl. Electrochem.* 3 (1973) 137.
- [12] J. Li, J. Jiang, H. He, Y. Sun, *J. Mater. Sci. Lett.* 21 (2002) 939.
- [13] F. Erler, C. Jakob, H. Romanus, T. Lampke, *Electrochim. Acta* 48 (2003) 3063.
- [14] D. Thiemi, A. Bund, *Surf. Coat. Technol.* 202 (2008) 2976.
- [15] A. Hovestad, L.J.J. Janssen, *J. Appl. Electrochem.* 25 (1995) 519.
- [16] E.A. Pavlatou, M. Raptakis, N. Spyrellis, *Surf. Coat. Technol.* 201 (2007) 4571.
- [17] R. Vittal, H. Gomathi, K.J. Kim, *Adv. Colloid Interf. Sci.* 119 (2006) 55.
- [18] D. Aslanidis, J. Fransaer, J.P. Celis, *J. Electrochem. Soc.* 144 (1997) 2352.
- [19] L. Stappers, J. Fransaer, *J. Electrochem. Soc.* 153 (2006) C472.
- [20] C. Dedeloudis, J. Fransaer, J.P. Celis, *J. Phys. Chem. B* 104 (2000) 2060.
- [21] G. Vidrich, J.-F. Castagnet, H. Ferkel, *J. Electrochem. Soc.* 152 (2005) C294.
- [22] E.A. Pavlatou, M. Stroumbouli, P. Gyftou, N. Spyrellis, *J. Appl. Electrochem.* 36 (2005) 385.
- [23] J.P. Bonino, S. Loubiere, A. Rousset, *J. Appl. Electrochem.* 28 (1998) 1227.
- [24] J. Amblard, M. Froment, N. Spyrellis, *Surf. Technol.* 5 (1977) 205.
- [25] J. Amblard, I. Epelboin, M. Froment, G. Maurin, *J. Appl. Electrochem.* 9 (1979) 233.
- [26] J. Amblard, M. Froment, *Faraday Discuss. Faraday Symp.* 12 (1978) 136.
- [27] J. Amblard, M. Froment, G. Maurin, N. Spyrellis, *J. Microsc. Spectrosc. Electron.* 6 (1981) 311.
- [28] S. Abel, H. Freimuth, H. Lehr, H. Mensinger, *J. Micromech. Microeng.* 4 (1994) 47.
- [29] A. McCormack, M.J. Pomeroy, V.J. Cunnane, *J. Electrochem. Soc.* 150 (2003) C356.
- [30] S.W. Banovic, K. Barmak, A.R. Marder, *J. Mater. Sci.* 34 (1999) 3203.
- [31] J. Amblard, G. Maurin, D. Mercier, N. Spyrellis, *Scripta Metall.* 16 (1982) 579.
- [32] J. Fransaer, J.P. Celis, J.R. Ross, *J. Electrochem. Soc.* 139 (1992) 413.
- [33] E.S. Chen, G.R. Lakshminarayanan, F.K. Sautter, *Met. Trans.* 942 (1971) 937.
- [34] L. Benea, P.L. Bonora, A. Borello, S. Martelli, *Wear* 249 (2002) 995.
- [35] S. Trasatti, *Electrochim. Acta* 36 (1991) 225.
- [36] J.B. Steltzer, R. Niltzschse, J. Caro, *Chem. Eng. Technol.* 28 (2005) 182.